Pedosphere **27**(6): 1037–1048, 2017
doi:10.1016/S1002-0160(17)60447-8
ISSN 1002-0160/CN 32-1315/P

Published by Elsevier B.V. and Science Press

PEDOSPHERE

www.elsevier.com/locate/pedosphere

Hydrological Responses and Flow Pathways in an Acrisol on a Forested Hillslope with a Monsoonal Subtropical Climate

Lars-Erik SØRBOTTEN[1], Jannes STOLTE[2,*], WANG Yanhui[3] and Jan MULDER[4]

[1] *Norconsult AS, N-1338 Sandvika (Norway)*
[2] *Norwegian Institute of Bioeconomy Research (NIBIO), N-1430 Aas (Norway)*
[3] *Research Institute of Forest Ecology, Environment and Protection, Chinese Academy of Forestry, Beijing 100091 (China)*
[4] *Department of Environmental Sciences, Norwegian University of Life Sciences, N-1432 Aas (Norway)*

(Received February 27, 2015; revised July 7, 2017)

ABSTRACT

The nature of subsurface flow depends largely on hydraulic conductivity of the vadoze zone, permeability of the underlying bedrock, existence of soil layers differing in hydraulic properties and macropore content, soil depth, and slope angle. Quantification of flow pathways on forested hillslopes is essential to understand hydrological dynamics and solute transport patterns. Acrisols, with their argic Bt horizons, are challenging in this respect. To further elucidate flow pathways of water and short-term variability of soil moisture patterns in Acrisols, a field study was conducted on a forested hillslope in a sub-catchment of the Tie Shan Ping (TSP) watershed, 25 km northeast of Chongqing City, China. This catchment is covered by a mixed secondary forest dominated by Masson pine (*Pinus massoniana*). Soil saturated hydraulic conductivity (K_{sat}) was significantly reduced at the interface between the AB and Bt horizons (2.6×10^{-5} *vs.* 1.2×10^{-6} m s^{-1}), which led to that the flow volume generated in the Bt horizon was of little quantitative importance compared to that in the AB horizon. There was a marked decrease in porosity between the OA and AB horizons, with a further decrease deeper in the mineral subsoil. Especially, the content of soil pores > 300 μm was higher in the AB horizon (14.3%) than in the Bt horizon (6.5%). This explained the difference in soil K_{sat} values. This study showed that Bt horizon had limited water transport capability, forcing part of the infiltrated rainwater as interflow through the OA and AB horizons. Thus, the topsoil responded quickly to rainfall events, causing frequent cycles of saturation and aeration of soil pores.

Key Words: dye tracer, hillslope hydrology, hydraulic conductivity, preferential flow, soil pores, subsurface lateral flow

Citation: Sørbotten L-E, Stolte J, Wang Y H, Mulder J. 2017. Hydrological responses and flow pathways in an Acrisol on a forested hillslope with a monsoonal subtropical climate. *Pedosphere*. **27**(6): 1037–1048.

INTRODUCTION

The nature of subsurface flow in soils depends largely on the hydraulic conductivity of the vadoze zone, permeability of the underlying bedrock, existence of soil layers differing in hydraulic properties and macropore content, soil depth, and slope angle (Lehmann *et al.*, 2007). The ratio of vertical and lateral water transport depends on slope angle and the degree of the anisotropy with respect to hydraulic conductivity (*e.g.*, Zaslavsky and Rogowski, 1969; Ritsema *et al.*, 1998; Elsenbeer, 2001). The rate of downhill-directed sub-surface water flow is not only determined by differences in vertical hydraulic conductivity between the diagnostic soil horizons, but also may depend on the vertical and lateral hydraulic conductivity of the soil horizons themselves (*e.g.*, Bathke and Cassel, 1991; Ritsema *et al.*, 1998). In addition, the connectivity of a preferential flow network is an important factor in flow-path development (*e.g.*, Chappell and Sherlock, 2005; Anderson *et al.*, 2009; Kim, 2014). As a result, water transport patterns in sloping terrain are difficult to predict (McGlynn *et al.*, 2002).

Traditional studies evaluating the impact of forest on runoff largely rely on the paired catchment approach, in which statistical relations for catchment outlet responses (*e.g.*, peak flow) between paired catchments are established (*e.g.*, Zégre *et al.*, 2010). However, to elucidate more detailed processes, Bruijnzeel (2004) stated that there was a distinct need to supplement the paired catchment approach with process-based measuring and modelling techniques. Based on a study in the humid tropics, Chappell and Sherlock (2005) concluded that there was insufficient information to allow simple generalizations about the magnitude and direction of water movement within specific

*Corresponding author. E-mail jannes.stolte@nibio.no.

soil groups. Such generalizations need to be based on a much greater set of hillslope experiments than that is currently available.

The macropore fraction is a major factor in determining the distribution of soil water on hillslopes (Noguchi *et al.*, 2001; Beven and Germann, 2013). The importance of preferential flow in macropore networks increases with soil moisture content (Bronstert and Plate, 1997; Ridolfi *et al.*, 2003), and it can become a dominant factor over matrix hydraulic conductivity during stormflow (Cheng, 1988; Noguchi *et al.*, 2001; Sidle *et al.*, 2001). Tromp-van Meerveld and Weiler (2008) found that inclusion of preferential flow in hillslope models produced simulation results that more closely matched the observed ranges of water table responses. Although it has been shown that antecedent soil moisture is an important control for flow pathway distribution (Longobardi *et al.*, 2003; Hardie *et al.*, 2011), its importance may be limited in systems with small variations in antecedent soil moisture. According to Kampf (2011), soil moisture values often occur within season-specific preferred small ranges, particularly in quickly drained soils. Tromp-van Meerveld and McDonnell (2006) showed the importance of soil depth in understanding the relations between soil moisture, transpiration, and vegetation patterns.

Overland flow is a potential pathway in forests in the humid Acrisol-dominated landscape in the tropics and subtropics (Elsenbeer, 2001). Under protective forest cover, water retention and transport on hillslopes in Acrisol-dominated landscapes are complicated by the presence of an argic Bt horizon below porous surface horizons. The argic Bt horizon is characterized by reduced permeability restricting internal soil drainage (WRB, 2006). Acrisols cover 1 000 million ha worldwide and are the dominant soil type in large parts of South China, Malaysia, Sumatra (Indonesia), and Southeast USA (WRB, 2006). Preferential flow, vertical as well as lateral, is very common in forested Acrisols in Southwest China, as a result of a high macropore density in the surface soil horizons mainly due to cracks formed by tree roots and soil fauna (Cheng *et al.*, 2009) and relatively high stone content. The soil macropores exert a stronger influence on the saturated hydraulic conductivity (K_{sat}) than the total porosity (Chen and Shi, 2005).

Elsenbeer (2001) suggested that the loss of nutrients, such as nitrate and potassium, must be higher in areas with widespread overland flow, because this pathway is essentially a shortcut to the stream channel that bypasses the sub-soil where a significant proportion of nutrient recycling occurs. He concluded that nutrient input-output studies in tropical rainforests on Acrisols, conducted without proper hydrological consideration, are likely to yield bias. The difficulty in predicting surface runoff in Acrisols, except where it is associated with channels, and the occurrence of return flow, poses a monitoring problem for overland flow. Van der Heijden *et al.* (2013) highlighted the importance of proper calibration of hydrological models using both soil water content data and tracing experiments when computing nutrient input-output budgets in a poor and acidic Alumic Cambisol under a 30-year-old beech stand in France. Zhang *et al.* (2004) concluded that preferential flow, representing the important influence of forest on runoff generation, is rarely studied in China. In the few existing studies, Cheng *et al.* (2009) reported that peak surface runoff is more extreme when preferential flow occurs, indicating that preferential flow has a significant effect on the peak surface runoff. The rainfall amount influences duration, peak discharge, and total discharge of preferential flow, whereas the duration of preferential flow also is affected by the duration of the rainfall event (He *et al.*, 2005). Cheng *et al.* (2009) attributed the occurrence of preferential flow to differences in soil properties between consecutive soil horizons. For example, textural differences between horizons influence soil water retention and conductivity characteristics of the soil, and thus infiltration behavior. In Acrisols under broadleaved forests of the Simian Mountains, Chongqing, Southwest China, Wang *et al.* (2010) reported radii of the macropores in the soil profile ranging from 0.3 to 3.0 mm (average: 0.48 mm) and macroporosities of 6.3%–10.5%. In forested Acrisols of the upper reaches of the Minjiang River (Sichuan Province, China), the radii of macropores ranged from 0.3 to 2.4 mm, with an average of 0.84 mm (Shi *et al.*, 2005).

The current lack of detailed quantitative information on infiltration capacity of subtropical and tropical forest soil, soil hydraulic conductivity profiles with depth, and soil water retention and storage capacities necessitates systematic sampling campaigns (Bruijnzeel, 2004). The present study, which forms part of a study to quantify nitrogen (N) transport and nitrous oxide (N_2O) emissions from forested areas in subtropical China, seeks to elucidate the flow pathways of water, and spatial and temporal variability of soil moisture patterns, in response to rain episodes on forested hillslopes.

The objectives of this study were to (i) identify the water flow pathways in an Acrisol on a forested hillslope with a well-developed argic Bt horizon, (ii) identify the parameters controlling water flow path-

ways, and (iii) quantify the temporal variation in soil moisture content in the surface soil horizons overlying the argic Bt horizon in response to rainfall. It was hypothesized that the vertical infiltration of water in the argic Bt horizon was restricted due to its lower water conductivity relative to the overlying topsoil, causing lateral preferential flow. This causes relatively rapid shifts between saturated and unsaturated conditions in the organic matter-rich topsoil, which is of crucial importance for redox sensitive biogeochemical processes (*e.g.*, N_2O production).

MATERIALS AND METHODS

Study site

The research was conducted on a hillslope in a sub-catchment of the Tie Shan Ping (TSP) watershed (Chen and Mulder, 2007; Larssen *et al.*, 2011). The sub-catchment, 4.64 ha in size, is situated in a protected forest park approximately 25 km northeast of Chongqing City, China. The catchment is covered mainly by relatively dense secondary mixed forest dominated by Masson pine (*Pinus massoniana*). The dominant soil type on the hillslope, located on a sandstone ridge, is a yellow mountain soil, classified as Orthic Acrisol, with a well-developed argic Bt horizon at about 20 cm soil depth. The average slope is 28%. The groundwater discharge zone (GDZ) at the foot of the hillslope, with seven terraces, consists of Cambisols, developed in colluvial deposits (Fig. 1). Although used for vegetable production for a limited period in the 1960s, these terraces have been unmanaged during at least four decades and are now covered by grasses, bracken and shrubs. The GDZ drains into a pond just below the study area. In the monsoonal rainy season (May–September), the groundwater table in the GDZ is generally near the surface, and ponding may occur during intensive rain episodes.

Besides having the argic Bt horizon, the Acrisol on the hillslope is characterized by a thin O horizon (+2–0 cm) of partly decomposed litter. Below this, there is an A horizon (0–5 cm) and a AB horizon (5–17 cm). The Bt horizon is divided in a Bt1 horizon (17–27 cm) and a Bt2 horizon (> 27 cm). The AB, Bt1, and Bt2 horizons are homogenous, but locally they contain fragments of regolithic sandstone of variable size, as well as small fragments of brick (except Bt2) from human activities. Below the Bt2 horizon, there is a gradual transition to the C (or R) horizon, consisting of weathered regolithic sandstone and regolith. The O and A horizons are considered one layer in this study, and referred to as OA horizon.

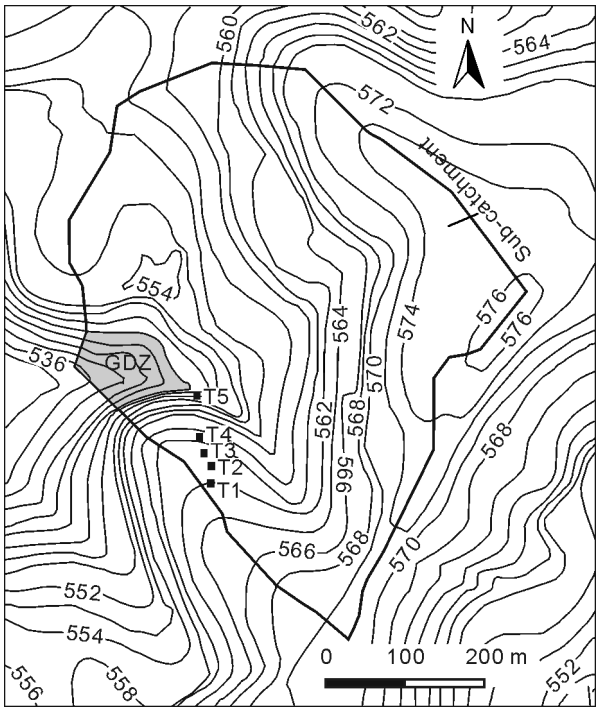

Fig. 1 Map of the study site, a sub-catchment in the Tie Shan Ping (TSP) watershed, Chongqing, China, with five profiles (T1–T5) along a transect perpendicular to contour lines and the groundwater discharge zone (GDZ) indicated.

Climate

Rainfall and temperature data were recorded at 5-min intervals from May 2009 until December 2010, using a WeatherHawk 232 weather station situated on a rooftop approximately 750 m from the study site. Based on (i) the amount of precipitation and (ii) the measured data on soil moisture content and runoff, six rainfall events were selected (Fig. 2) with a total precipitation over 20 mm each for detailed analysis.

Soil analysis

Soil water retention characteristics (θ_h) (cm^3 cm^{-3}) were determined at the Norwegian University of Life Sciences, using soil cores taken from five soil profiles (T1–T5) along a transect perpendicular to the contour lines (Fig. 1). The transect length was approximately 50 m from the top to the foot of the hillslope, with an elevation difference of approximately 14 m. In each of the five profiles, steel cylinders of 100 cm^3 (diameter = 5.9 cm, height = 3.75 cm) were used to take undisturbed soil samples (two replicates) at depths of 3.5, 10, 25, and 50 cm. The θ_h values were measured with a sandbox and adjustable hanging water column (at pressures of −1 and −5 kPa) and pressure plate extraction (at −10 and −50 kPa), both using 100-cm^3

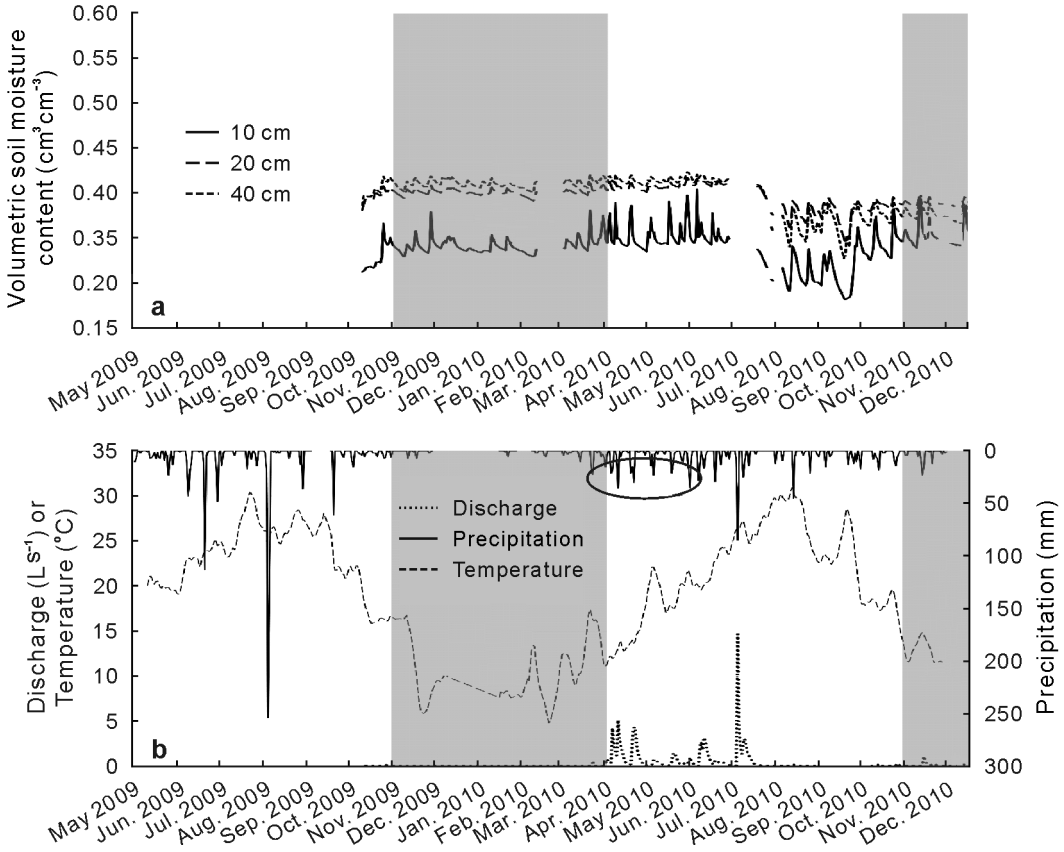

Fig. 2 Volumetric soil moisture content at 10, 20, and 40 cm of profile T3 (a) and daily precipitation, mean stream-water discharge, and mean temperature (b) from May 2009 to December 2010 in the Tie Shan Ping watershed, Chongqing, China. The temperature values are 10-d moving averages. Data are adapted from Zhu *et al.* (2013a, b). The six rainfall events used for detailed analysis of flow pathways are highlighted by circles. Dry seasons are highlighted by grey colour.

undisturbed samples. Disturbed soil samples in plastic rings (radius = 19 mm, height = 13 mm) were used for pressure plate extractions at −100, −300, and −1 500 kPa (van Reeuwijk, 2002). Porosity (cm^3 cm^{-3}) was calculated from the weight difference between saturated and oven-dried (105 °C for 24 h) undisturbed samples in the 100-cm^3 steel rings. Dry bulk density was calculated from the dry weight of the samples. Samples were used for soil texture measurements using the sieve method for coarse material (> 2 mm) and the pipette method for the fine earth fraction.

Values for K_{sat} (m s^{-1}) were determined in undisturbed soil samples, using steel cylinders of 200 cm^3 (diameter = 7 cm, height = 5.1 cm). Soils were sampled (in triplicate) from the combined A/AB horizon and the Bt horizon. Measurements were done in a field laboratory using a constant-head set-up (Stolte, 1997).

To describe the water retention curve of the soil, the Mualem-Van Genuchten (MvG) equation was used (van Genuchten, 1980), following model parameter optimization. This was done using the measured θ_h and K_{sat} data and the curve fitting program RETC, version 6.02 (Van Genuchten *et al.*, 1992).

Pore size distribution was estimated from the soil water retention curves assuming the following relationship between capillary rise (h_c, m) and pore radius (r, m):

$$h_c = (2\gamma \cos\alpha)/r\rho_w g \quad (1)$$

where γ is the surface tension of water (N m^{-1}), α is the liquid-solid contact angle (assumed to be zero for water), ρ_w is the water density (g m^{-3}), and g was the gravitational acceleration (m s^{-2}) (Hillel, 1980). Pore radius (m) in soils at 20 °C was solved as $r \approx 0.15/|h_c|$.

Stream-water discharge and in situ soil moisture dynamics

At the catchment outlet, surface runoff was measured using an H-flume with an ultrasonic water height sensor connected to a data-logger. For profile T3, the *in situ* volumetric soil moisture content, θ (cm^3 cm^{-3}), was measured using dielectric permittivity sensors (Hydra Probe II, Stevens Water Monitoring Systems Inc., USA). The probes were installed horizontally at depths of 10, 20, and 40 cm, and soil moisture was

logged at 10-min intervals using a Campbell CR200 data logger (Campbell Scientific Inc., USA). For soil water storage estimations, soil moisture values from the 10-cm sensor were assumed to apply to 0–15 cm, values from the 20-cm sensor to 15–30 cm, and values from the 40-cm sensor to 30–50 cm.

The change in volumetric soil moisture contents in individual soil layers per rainfall event, $\Delta\theta$ (cm^3 cm^{-3}), was calculated by the final soil volumetric moisture content at the end of the rainfall event minus antecedent volumetric soil moisture content (θ_{ant}). An event was defined as starting at first rainfall and ending when the stream-water discharge at the catchment outlet was back to the pre-rainfall level. Maximum change in volumetric soil moisture content, $\Delta\theta_{max}$ (cm^3 cm^{-3}), was the maximum volumetric soil moisture content per individual soil layer during the rainfall event minus θ_{ant}. Both the difference in soil water storage between the end of the event and antecedent conditions, ΔS (mm), and maximum change in soil water storage, ΔS_{max} (mm), were calculated from $\Delta\theta$ and $\Delta\theta_{max}$, respectively, and integrated over the depth range of the soil. Thus, ΔS was calculated by the equation:

$$\Delta S = \Sigma(\Delta\theta_i \times M_i) \quad (2)$$

where $\Delta\theta_i$ is the change in volumetric soil moisture content (cm^3 cm^{-3}) in soil layer i and M_i is the thickness of the relevant depth range in soil layer i (cm). ΔS_{max} was calculated correspondingly using $\Delta\theta_{max}$.

Tracer experiment

A dye tracer experiment was performed at two plots (1 m × 1 m each), one at the top of the slope ("upper", near profiles T1 and T2) and one at the foot of the hillslope ("lower", near profile T5), using infiltration of brilliant blue FCF solution (Flury and Flühler, 1994; Flury and Wai, 2003). The soil near profiles T1 and T2 was a silty clay loam with the argic Bt horizon, whereas the soil near profile T5 was a silt loam (colluvium) (Zhu *et al.*, 2013b). Both the upper and the lower plots, with slopes of 15% and 10%, respectively, were cleared of ground vegetation by clipping at the soil surface. Ten millimeters of brilliant blue FCF solution (4 g brilliant blue L^{-1}) were applied at the lower half of each plot (0.5 m perpendicular to the contour lines × 1 m wide). Subsequently, the full 1 m × 1 m plots were irrigated with approximately 80 mm of clean tap water over a 6-h period (rainfall intensity of 13.3 mm h^{-1}). This amount was based on a study from Wang *et al.* (2013), who presented rainfall intensities for the Chongqing area during the years 2009–2011. Their values varied from 1.5 to 72 mm h^{-1}, with a maximum daily amount of 59.3 mm. Using the dye tracer, we assessed the effect of infiltration of rainwater upslope of the tracer application on the direction of tracer movement. Both brilliant blue application and subsequent irrigation were performed homogeneously using back-mounted manual sprayers. Application started at around 11:30 a.m. on June 30 for both plots. The plots were excavated on the following day (around 22 h after application for the upper plot and 27 h for the lower plot). For an estimate of potential penetration depth, available porosity (pore space) (φ_a, cm^3 cm^{-3}) was calculated as the difference between total porosity (φ, cm^3 cm^{-3}) and antecedent volumetric soil moisture content (θ_{ant}, cm^3 cm^{-3}) of profile T3:

$$\varphi_a = \varphi - \theta_{ant} \quad (3)$$

The average φ_a was weighted with respect to the relevant depth ranges for each soil water sensor:

$$\text{Average } \varphi_a = \Sigma(\varphi_{a,i} \times M_i)/\Sigma M_i \quad (4)$$

where $\varphi_{a,i}$ is the available porosity in soil layer i (cm^3 cm^{-3}) and M_i is the thickness of the relevant depth range in soil layer i (cm).

RESULTS

Climate and runoff

The summer of 2010 was relatively dry (Table I) and rainfall occurred mostly as intensive rainstorms (up to 385 mm during 41 h on August 3–5, 2009). In particular, in August and September 2010, the climate was dry (Table I). This was reflected by the volumetric soil moisture content, which showed a decrease at all depths from August 2010, and by the stream-water discharge, which was zero until a small rainfall event in December 2010 (Fig. 2).

Between April 6 and May 31, 2010, we selected all rainfall events (six in total) with a total precipitation over 20 mm each (29–66 mm), varying in duration from almost 10 to over 50 h (Table II). These events produced measurable stream-water discharge, which was an important criterion for further analysis. Unfortunately, the large event in July 2010 could not be included in this selection, because the soil moisture measurement equipment malfunctioned. Events, not producing discharge (Fig. 2), indicated that all precipitation was lost through interception, infiltration, evapotranspira-

TABLE I

Rainfall and daily temperature from May 2009 to November 2010 in the Tie Shan Ping watershed, Chongqing, China[a)]

Month	N[b)]	Precipitation		Daily temperature		
		Total	Normal[c)]	Mean	Minimum	Maximum
		mm		°C		
May 2009	31	114	159	19.9	15.6	24.7
Jun. 2009	30	284	166	23.8	19.1	29.2
Jul. 2009	31	62	171	26.8	19.3	32.0
Aug. 2009	31	449	138	26.4	22.0	31.1
Sep. 2009[d)]	17	70	149	22.9	17.9	28.1
Oct. 2009	31	75	96	17.5	13.9	24.9
Nov. 2009	29	19	53	10.9	2.9	18.6
Dec. 2009[d)]	0	–	26	–	–	–
Jan. 2010[d)]	13	6	20	8.0	4.9	9.9
Feb. 2010[d)]	21	13	21	8.5	3.7	17.3
Mar. 2010	31	79	37	12.8	5.7	24.3
Apr. 2010	30	182	102	14.7	8.3	23.9
May 2010	31	128	159	19.7	15.3	26.2
Jun. 2010	30	165	166	22.3	16.7	27.9
Jul. 2010	31	143	171	27.6	21.2	31.9
Aug. 2010	31	101	138	27.2	19.4	33.1
Sep. 2010	30	80	149	23.2	16.5	31.5
Oct. 2010	31	95	96	17.0	9.4	21.1
Nov. 2010	30	77	53	12.6	9.8	17.0

[a)] Cited from Zhu *et al.* (2013a).
[b)] Number of recording days per month.
[c)] Normal precipitation based on monthly averages for the 30-year period 1961–1990 for Chongqing City, approximately 10 km from the study site.
[d)] Months with missing values for three or more days.

tion, and/or leaching to deeper soil layers.

Discharge measurements for the events yielded total durations between 73 and 210 h. Average precitation intensity for the six events varied from 0.9 to 4.7 mm h^{-1}, whereas peak intensity was from 5 to 15 mm h^{-1}. The average runoff coefficient (percentage of precipitation that appeared as runoff) for the six studied events in the observation period was 31%, varying from 8% to 53%. The annual average runoff coefficient was 25% (data not shown). The water balance deficit (here defined as the percentage of precipitation not recovered as runoff and storage change in the soil on the hillslope) for the six events varied from 44.5% to 94.6%. There was an abrupt drop in runoff from April to May 2010, with a corresponding drop in runoff coefficient and an increase in water balance deficit (Table II). The increasing deficit can be explained mostly by the increasing evapotranspiration, but also by the change in soil water storage in the GDZ at the foot of the hillslope and/or seepage in the underlying sandstone. The drop in soil moisture content from August 2010 onwards can be explained by lower rainfall input and higher evapotranspiration output in this dry year compared with normal years. From August 2010, there was hardly any stream-water discharge produced (Fig. 2), compared with the early stage of the wet season.

Soil

Except in the GDZ and at the foot of the hillslope, the soils had Acrisol characteristics, including the Bt horizon with illuviated clay. However, they lacked a clay-eluviation layer (Table III), probably due to the truncation caused by erosion (Driessen *et al.*, 2001). Consequently, the clay content in the AB and Bt horizons did not differ significantly ($P > 0.05$), using Tukey's test (Table III).

There was a substantial and significant ($P < 0.01$) difference in K_{sat} between the AB and B horizons (Table IV), with the average K_{sat} being 16 times greater in the AB horizon than in the Bt horizon. Values of K_{sat} for the AB and B horizons did not differ significantly between the foot of the hillslope (T5) and the plots fu-

TABLE II

Meteorological and hydrological data of six major rainfall events producing stream-water discharge between April 6 and May 31, 2010 in the Tie Shan Ping watershed, Chongqing, China

Event	Event date	Duration		Precipitation	Precipitation intensity		Runoff	ΔS[b)]	Water balance deficit[c)]	Runoff coefficient[d)]
		Event[a)]	Rainfall		Average	Maximum				
		h		mm	mm h^{-1}		mm		%	
1	Apr. 6	118.5	27.6	39	1.4	7.0	17.6	0.2	54.0	45
2	Apr. 10	112.8	9.7	45	4.7	9.0	23.7	1.3	44.5	53
3	Apr. 20	209.6	44.3	66	1.5	12.0	31.9	−1.3	53.5	48
4	May 6	96.0	31.4	29	0.9	14.0	4.5	−0.3	85.6	15
5	May 18	73.3	32.1	38	1.2	5.0	6.0	3.7	74.4	16
6	May 31	120.3	50.3	59	1.2	5.0	4.6	−1.5	94.6	8

[a)] Starts at first rainfall and ends when stream-water discharge is back to pre-rainfall levels.
[b)] Difference in soil water storage between the end of the event and antecedent conditions.
[c)] Percentage of precipitation not recovered as runoff and storage change in the soil on the hillslope.
[d)] Percentage of precipitation that appeares as runoff.

TABLE III

Soil texture[a] for five profiles (T1–T5) on the hillslope in the Tie Shan Ping watershed, Chongqing, China

Fraction	Soil horizon	n	Percentage of the fine earth fraction (< 2 mm)				
			Mean	SD[b]	Minimum	Median	Maximum
			%				
Sand	AB	5	17.6	7.7	11.4	15.8	30.6
	Bt	5	18.1	11.3	8.6	11.0	30.8
Silt	AB	5	56.3	4.8	50.8	56.0	61.4
	Bt	5	54.4	5.0	50.3	52.0	61.7
Clay	AB	5	26.2	6.5	18.6	26.4	36.2
	Bt	5	27.6	8.6	18.9	28.5	39.4

[a]The coarse fraction (> 2 mm) varied from 1% to 28% and from 2% to 22% in the AB and B horizons, respectively, with median values of 8% for both horizons.
[b]Standard deviation.

further up on the hill (T1–T4; data not shown).

Soil water retention curves (Fig. 3) showed a difference between the OA horizon and the mineral horizons below, but not between the AB and Bt horizons. There was a marked decrease in porosity from the OA horizon (0.49 cm^3 cm^{-3}) to the mineral horizons below, but the decrease with depth was less pronounced in the mineral subsoil (AB through Bt2 horizons where the porosity was about 0.44 to 0.43 cm^3 cm^{-3}) (Table V, Fig. 4). Pore size distributions estimated from the soil water retention curves (Fig. 3) indicated a significantly greater proportion of the largest pores and a lesser proportion of the smallest pores in the AB horizon than in the Bt horizon.

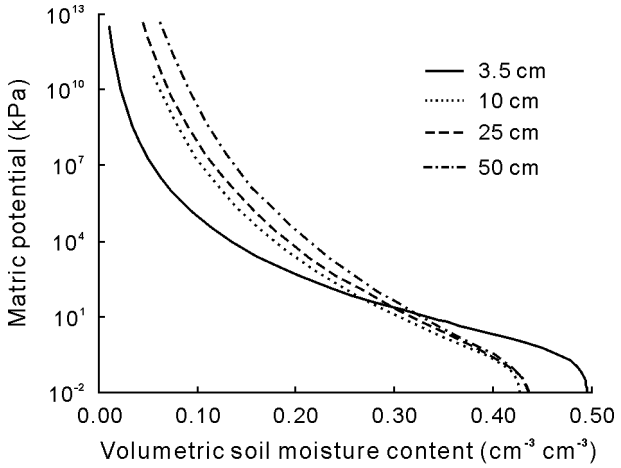

Fig. 3 Soil water retention curves according to the van Genuchten-Mualem equation after parameter optimization estimated from mean observed values for each measured depth: depths of 3.5, 10, 25, and 50 cm correspond with the OA, AB, Bt1, and Bt2 horizons, respectively.

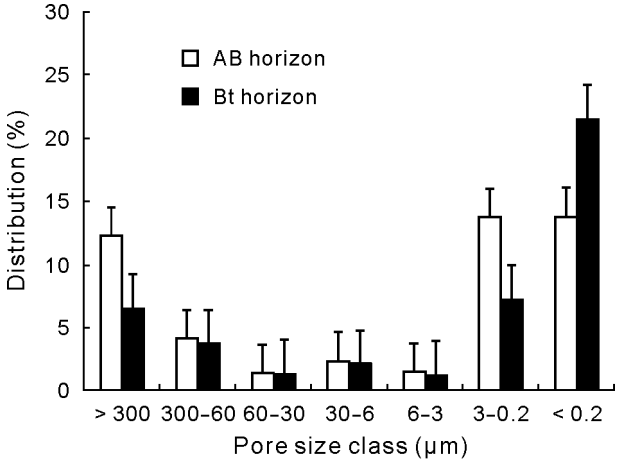

Fig. 4 Distribution of pore size classes by soil horizon in the Tie Shan Ping watershed, Chongqing, China. Values are averages for the five soil profiles (T1–T5) obtained from soil water retention curves. Pore size classes of > 300 and < 0.2 µm both differed at $P < 0.05$ using a 2-sample t-test. The 1-µm pore size class (calculated from the −300 kPa pressure) was excluded from the estimation due to measurement errors.

In situ soil moisture dynamics

The variation in volumetric soil moisture content was relatively limited during the summers of 2009 and 2010, but the volumetric soil moisture content at all depths showed a consistent decrease in the second part of the wet season (from July onwards) (Fig. 2). The drying of the soil from July was likely caused by the precipitation deficit relative to the demand by evapotranspiration (despite it being the tail of the wet season). However, there was no clear difference in soil moisture between the first part of the wet season and the dry (winter) season (Fig. 2). Although it can be assumed that the equipment became unreliable after the large event at the beginning of July, the measured re-

TABLE IV

Saturated hydraulic conductivity (K_{sat})[a] by soil horizon on the hillslope in the Tie Shan Ping watershed, Chongqing, China

Soil horizon	n	K_{sat}				
		Mean	SD[b]	Median	Minimum	Maximum
		$m\ s^{-1}$				
AB	28	2.6×10^{-5}	5.3×10^{-5}	8.4×10^{-6}	2.7×10^{-8}	2.7×10^{-4}
Bt	23	1.2×10^{-6}	2.0×10^{-6}	3.8×10^{-7}	9.7×10^{-9}	6.8×10^{-6}

[a]Values are grouped for all investigated soil profiles (T1–T5).
[b]Standard deviation.

TABLE V

Total porosity (φ) and antecedent volumetric soil moisture content (θ_{ant}) of profile T3 at start of the dye experiment, and estimated available porosity (φ_a), both for individual layers and weighted average for the profile

Depth	φ	θ_{ant}	φ_a	Average φ_a
cm			$cm^3\ cm^{-3}$	
0–15	0.44	0.28	0.16	0.10
15–30	0.44	0.36	0.08	
30–50	0.43	0.36	0.07	

sult after restart of the equipment showed the volumetric soil moisture content that followed the final measured result just before the gap in measurements. In addition, from August onwards hardly any discharge was measured. The discharge measurement was a stand-alone device, and had no measurement gaps during 2010. This strengthened our observation that the precipitation amount did not exceed the sum of interception, evapotranspiration, and seepage for this period.

The six events had only small differences in θ_{ant} at any given depth, but the values were significantly smaller at 10 cm than at greater soil depth. By contrast, the $\Delta\theta_{max}$ value was significantly greater at 10 cm than at 20 and 40 cm (Table VI). The value of $\Delta\theta_{max}$ during all six events amounted to 0.37 $cm^3\ cm^{-3}$ at all depths. Soil moisture response to rainfall started in the deepest horizon and proceeded upwards through the horizons (Table VI).

Tracer experiment

In the upper plot, the tracer reached about 20–25 cm depth below the soil surface (with some spots visible at 30 cm depth). In addition, a considerable fraction of the dye extended about 20 cm downslope of the application area (Fig. 5). Dye had some tendency to concentrate around and below small rock fragments in the profile. Available pore space for dye transport was estimated at a weighted average of 12% (Table V).

In the lower plot on the hillslope (Fig. 5), the average depth of the infiltration front was at about 30 cm, somewhat deeper than that in the upper plot. In addition, the lateral movement outside the application area was limited to about 5 cm.

DISCUSSION

Although the soil moisture response to precipitation occurred in the Bt horizon first in the Acrisol studied, indicating the existence of vertical preferential flow pathways through the OA and AB horizons (Rosenbaum *et al.*, 2012), the increase in volumetric soil moisture content in the Bt1 and Bt2 horizons was small (Table VI). This indicates that the flow volume generated in the Bt horizon is of little quantitative importance compared to that in the AB horizon. The dye infiltration pattern in the Acrisol (upper plot on the hillslope) gave a clear indication that the majority of the flow volume took place in the OA and AB horizons, partially vertically, but also as interflow laterally (about 20 cm outside of the dye application zone). This trend of lateral sub-surface transport of dye tracer was barely present in the lower plot at the foot of the hillslope. By contrast, the infiltration front in this plot reached about 30 cm depth, indicating nearly exclusively vertical transport. The slope was steeper (15%) at the upper than at the lower plot (10%), which might partly explain the lack of lateral sub-surface flow at the latter. Another possible reason for the difference in response was due to the differences in soil characteristics. Texture analysis for soil profile T5 showed a higher sand content and bulk density compared to soil profiles T1 and T2 (Zhu *et al.*, 2013b). The profile in

TABLE VI

Antecedent volumetric soil moisture content (θ_{ant}), maximum change in volumetric soil moisture content ($\Delta\theta_{max}$), maximum change in soil water storage (ΔS_{max}), and soil moisture response time for the six rainfall events in different soil layers[a)]

Event	θ_{ant}			$\Delta\theta_{max}$			ΔS_{max}				Soil moisture response time[b)]		
	10 cm	20 cm	40 cm	10 cm	20 cm	40 cm	0–15 cm	15–30 cm	30–50 cm	0–50 cm	10 cm	20 cm	40 cm
	$cm^3\ cm^3$						mm				hh:mm		
1	0.27	0.35	0.36	0.10	0.03	0.02	15.0	4.1	3.6	22.7	03:45	02:15	01:15
2	0.27	0.35	0.36	0.10	0.02	0.05	14.7	3.6	9.0	27.3	03:15	02:05	01:15
3	0.27	0.35	0.36	0.10	0.02	0.02	15.3	3.5	3.6	22.4	01:25	01:15	01:05
4	0.27	0.35	0.36	0.08	0.02	0.02	12.0	2.6	3.4	18.0	00:10	00:10	00:00
5	0.27	0.35	0.36	0.10	0.02	0.01	14.7	3.3	2.8	20.8	02:40	02:00	01:40
6	0.27	0.35	0.36	0.10	0.02	0.01	14.6	2.6	2.8	19.9	02:10	02:00	01:50

[a)] Soil moisture values from the 10-, 20-, and 40-cm sensors were assumed to apply to the 0–15 cm, 15–30, and 30–50 cm soil layers, respectively.

[b)] Time lapsed from rainfall event start to initial soil moisture response.

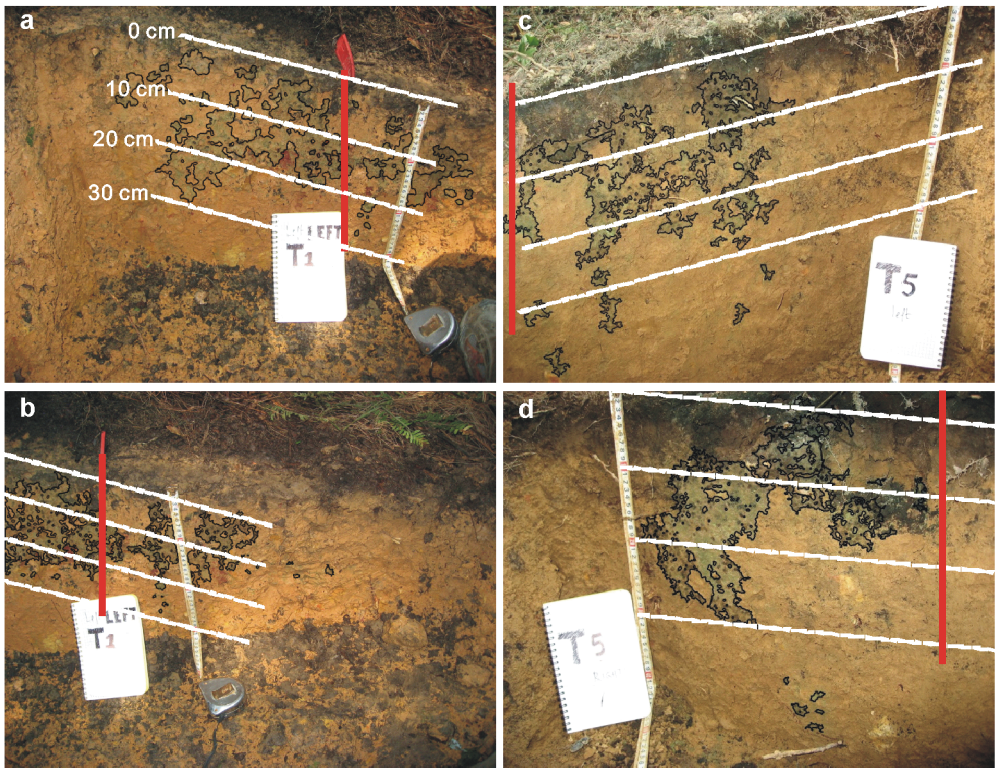

Fig. 5 Dye tracer penetration in the upper (a and b) and lower (c and d) plots. The upper plots are from the left side of the upslope pit near profile T1; the lower plots are from the left (c) and right (d) sides of the lower pit near profile T5. White dotted lines indicate depth and slope direction. The red bars indicate the lower part of the dye application area.

the lower plot was likely formed in part by colluvium material.

The difference in infiltration between the soil horizons in Acrisols were most likely associated with the greater proportion of the largest pores and the lesser proportion of the smallest pores in the AB horizon than in the Bt horizon (Fig. 4). The dye penetration was not homogenous, but concentrated in large pores, cracks, and around stone fragments, suggesting a dominance of macropore flow. For example, in the AB horizon, a large amount of root-derived pores occurred compared to the lower horizons. In a study at TSP, Zhang *et al.* (2008) also found a high concentration of fine roots, especially concentrated at 0–10 cm depth, with a density of 75 g m^{-3}. The maximum penetration depth of the dye reached the Bt2 horizon. This is in accordance with Laine-Kaulio *et al.* (2015), who found a maximum penetration depth to the BC horizon for a dye experiment in a forested hillslope on Haplic Podzol with sandy till. Obviously, the amount of dye solution applied can influence the penetration depth; total solution amount in this study was about 160% of the total free pore space volume (Table V). More solution added could have led to a deeper penetration of the dye and/or an increase in the lateral flow fraction.

Event 2, which had the highest average precipitation intensity of 4.7 mm h^{-1}, was the only event to produce substantially increased water content at 40 cm soil depth. Although this event did not have the highest maximum precipitation intensity, it might suggest that there was a pore space volume in the deeper soil, which was activated at an average precipitation intensity threshold (or more likely was activated over a certain threshold for soil moisture content of the top layer by development of preferential flow pathways). In addition, Cheng *et al.* (2009) found a positive correlation between rainfall amount over time and the occurrence of preferential flow. Lehman *et al.* (2007) presented a model to quantify the threshold relationship between precipitation intensity and outflow. Using the model, they could explain the measured variation in the relationship between rainstorm amount and subsurface flow by, among others, connecting macropores. Van Schaik *et al.* (2008) studied hillslope hydrology for a semi-arid catchment with Cambisols and Leptosols in Spain and found a fast response of percolation of water into the deeper layers. They concluded that this is caused by the existence of both matrix and macropore domains, where the macropore domain fills and empties rapidly and the matrix domain reacts more slowly.

In combination, *in situ* soil water, tracer and K_{sat} data in this study suggested that the dominant flow pathway was through the AB horizon (both vertically and laterally) rather than the deeper Bt horizon. Based on the occurrence of dye downslope of the application area, this indicated a preference for lateral flow at the hillslope, supported by the observation of ponding at the GDZ during intensive rainfall events (data not shown). This could also be seen in the average storage of around 65% of the precipitation in the 0–15-cm layer (AB horizon) of the six events (Table VI), and 20% in the 15–30-cm layer (Bt horizon). When extrapolating these values to the dye experiment, about 16 mm of the irrigated 80 mm water would reach the Bt horizon.

The significant difference in soil K_{sat} between the AB and Bt horizons (Table IV) was not reflected by the porosity values (total porosity of AB through Bt2 horizons of 0.44–0.43 cm^3 cm^{-3}). Yet, water transport characteristics are also influenced by pore size distributions (Arya *et al.*, 1999; Ghanbarian-Alavijeh and Hunt, 2012). The significantly higher proportion of the largest pore radii (> 300 μm) in the AB horizon and the increased prevalence of the smallest pore fraction (< 0.2 μm) in the Bt horizon, as shown in Fig. 4, could explain the observed differences in soil water storage (Table VI), soil water transport (Fig. 5), and soil K_{sat} values. This suggested that soil K_{sat} could be a proxy for the macropore distribution, and thus for estimating flow pathways at the hillslope. Distribution of existing pore networks or flow-induced connectivity between otherwise isolated pore structures may also be of importance and should be investigated in future research.

Although initial conditions, in particular antecedent soil moisture, have been shown to exert a significant control on flow distribution in other studies (Longobardi *et al.*, 2003; Hardie *et al.*, 2011), this is not the case in the TSP watershed. In accordance with Kampf (2011), the antecedent soil moisture showed little variation within seasons, thus limiting or even entirely negating its impact on stream flow response. The hillslope soils at TSP seemed to revert to such a preferred soil wetness state very quickly after a rainfall event. This preferred soil wetness state was slightly less than equilibrium soil water content at -10 kPa in the AB horizon and slightly more in the Bt horizon. The ΔS value averaged at 0.4% of precipitation (Table I), suggesting that the system quickly returned to the preferred soil moisture content after events and that the soil did not retain water in excess of the preferred soil wetness. With an antecedent soil moisture variability of less than 1% (Table VI), no prediction of event response or flow distribution from antecedent soil moisture conditions alone can be done. As indicated, there was a bottom upwards soil moisture response. In general, the soil layer of 30–40 cm had a response time of 1–2 h after start of the rainfall event (Table VI), after which the other layers followed in sequence from the bottom upwards with about 1-h intervals. Only Event 4 showed a different pattern, where the deeper layer responded almost instantaneously after the rainfall event started, and only minutes later was followed by the other soil layers. This might be due to the highest maximum intensity of this event compared to the other events.

The annual average runoff coefficient of 25% indicated that a large fraction of the precipitation did not reach the catchment discharge point, suggesting considerable water sinks as canopy interception, evapotranspiration, water storage change in the GDZ, and seepage to deeper layers. Studies of Chinese forests at similar latitudes and with similar vegetation indicate that annual actual evapotranspiration can range from 40% to over 70% of annual rainfall, and canopy interception can range from 15% to 30% (Wei *et al.*, 2005). In a parallel study, Wang (2012) conducted a monitoring campaign on evapotranspiration and interception; in this study, throughfall was measured at several spots in the study area, and four representative trees were selected for sap flow measurements. Results from this study confirmed that monthly evapotranspiration varied from 21% (June) to 87% (August) of rainfall in 2010 and could at times even exceed rainfall by up to 300% in months with little rainfall, such as in February 2011. The same study found that monthly canopy interception varied between 9% and 19% of rainfall, somewhat lower than the values published by Wei *et al.* (2005). Seepage may also explain part of the water balance of the area. Graham *et al.* (2010) stated that there was still lack of understanding of the contribution of deep seepage on hillslopes to the water balance of catchments. They concluded from their studies in a forested area in Oregon, USA, that deep seepage at the catchment scale averaged 21% of precipitation.

A possible explanation for the sudden drop in runoff from April to May 2010 (Table II, Fig. 2) was the increased evapotranspiration at the start of the growing season, following a temperature increase. However, while evapotranspiration data from Wang (2012), starting in May 2010, showed a substantial evapotranspiration increase from April to May in 2011, evapotranspiration was particularly low in May 2010 and was not likely sufficient to explain the sudden runoff changes from April to May 2010. Because soil water

storage showed no difference between April and May (Table II), the only explanation for the high water balance deficit can be the filling up of GDZ with water and partly the leakage of water in deeper layers. Soil moisture response in Event 4 (June 5, 2010) was much more rapid than that in other events, which may be explained by preferential pathways that temporarily allowed more rapid and deeper infiltration. However, there was no plausible explanation why this would occur in May, and not in April. The drop in volumetric soil moisture content in August 2010 was most likely caused by an increased evapotranspiration combined with a relatively low precipitation during this period.

CONCLUSIONS

Results of this study showed that subsurface flow happened in the topsoil as lateral interflow in the OA and AB horizons. The dye pattern in the upper experimental plot on the hillslope gave a clear indication that the majority of the flow volume took place in these horizons. Lateral flow in this plot occurred just above the Bt1 horizon. This indicated lateral sub-surface flow on top of the argic Bt horizon of the hillslope. Relatively fast sub-surface water transport downhill was supported by the occurrence of rapid ponding in the GDZ during intensive rainfall events. In contrast to the observed lateral transport in the upper soil plot on the hillslope, no such phenomenon was observed in the plot at the foot of the hillslope where soils had developed from colluvium. On average, around 20% of infiltrated water contributed to ΔS in the Bt horizon. Total ΔS of the six events for the 0–50 cm soil depth was 131 mm, of which about 25 mm reached the depth of 30–50 cm. This strengthened the observation that lateral flows prevailed over vertical infiltration. The most successful flow pathway predictor was saturated hydraulic conductivity, which was 16 times higher in the AB horizon than in the Bt horizon. The topsoil thus responded quickly to rainfall events, causing frequent cycles of saturation and aeration of soil pores, which was of crucial importance for redox sensitive biogeochemical processes (*e.g.*, N_2O production).

ACKNOWLEDGEMENT

This research is supported by the Norwegian Research Council (Nos. 193725/S30 and 209696/E10) and Chinese Academy of Science (CAS) (No. 209696/E10).

REFERENCES

Anderson A E, Weiler M, Alila Y, Hudson R O. 2009. Subsurface flow velocities in a hillslope with lateral preferential flow. *Water Resour Res.* **45**: W11407.

Arya L M, Leij F J, Shouse P J, van Genuchten M T. 1999. Relationship between the hydraulic conductivity function and the particle-size distribution. *Soil Sci Soc Am J.* **63**: 1063–1070.

Bathke G R, Cassel D K. 1991. Anisotropic variation of profile characteristics and saturated hydraulic conductivity in an Ultisol landscape. *Soil Sci Soc Am J.* **55**: 333–339.

Beven K, Germann P. 2013. Macropores and water flow in soils revisited. *Water Resour Res.* **49**: 3071–3092.

Bronstert A, Plate E J. 1997. Modelling of runoff generation and soil moisture dynamics for hillslopes and micro-catchments. *J Hydrol.* **198**: 177–195.

Bruijnzeel L A. 2004. Hydrological functions of tropical forests: not seeing the soil for the trees? *Agric Ecosyst Environ.* **104**: 185–228.

Chappell N A, Sherlock M D. 2005. Contrasting flow pathways within tropical forest slopes of Ultisol soils. *Earth Surf Process Landforms.* **30**: 735–753.

Chen F Q, Shi H. 2005. A primary study on the relation of soil macropore and water infiltration in evergreen broad-leaved forest of Jinyun Mountain. *J Southwest China Normal Univ* (*Nat Sci*) (in Chinese). **30**: 350–353.

Chen X Y, Mulder J. 2007. Indicators for nitrogen status and leaching in subtropical forest ecosystems, South China. *Biogeochemistry.* **82**: 165–180.

Cheng J D. 1988. Subsurface stormflows in the highly permeable forested watersheds of southwestern British Columbia. *J Contam Hydrol.* **3**: 171–191.

Cheng J H, Zhang H J, Zhang Y Y, Shi Y H, Cheng Y. 2009. Effects of preferential flow on soil-water and surface runoff in a forested watershed in China. *Front For China.* **4**: 132–139.

Driessen P, Deckers J, Spaargaren O, Nachtergaele F. 2001. Lecture Notes on the Major Soils of the World. Food and Agriculture Organization of the United Nations, Rome.

Elsenbeer H. 2001. Hydrologic flowpaths in tropical rainforest soilscapes—a review. *Hydrol Processes.* **15**: 1751–1759.

Flury M, Flühler H. 1994. Brilliant blue FCF as a dye tracer for solute transport studies—a toxicological overview. *J Environ Qual.* **23**: 1108–1112.

Flury M, Wai N N. 2003. Dyes as tracers for vadose zone hydrology. *Rev Geophys.* **41**: 1002.

Ghanbarian-Alavijeh B, Hunt A G. 2012. Unsaturated hydraulic conductivity in porous media: Percolation theory. *Geoderma.* **187-188**: 77–84.

Graham C B, Van Verseveld W, Barnard H R, McDonnell J. 2010. Estimating the deep seepage component of the hillslope and catchment water balance within a measurement uncertainty framework. *Hydrol Process.* **24**: 3631–3647.

Hardie M A, Cotching W E, Doyle R B, Holz G, Lisson S, Mattern K. 2011. Effect of antecedent soil moisture on preferential flow in a texture-contrast soil. *J Hydrol.* **398**: 191–201.

He F, Zhang H J, Shi Y H, Cheng J H, Qi S L, Pan L. 2005. Influence of rainfall factors on preferential flow in the granite region of the Three Gorges of the Yangtze River. *Trans Chin Soc Agr Eng* (in Chinese). **21**: 75–78.

Hillel D. 1980. Applications of Soil Physics. Academic Press, New York.

Kampf S K. 2011. Variability and persistence of hillslope initial conditions: A continuous perspective on subsurface flow response to rain events. *J Hydrol.* **404**: 176–185.

Kim S. 2014. Connectivity and topographic thresholds in bihourly soil moisture measurements along transects on a steep hillslope. *J Hydrol.* **512**: 563–574.

Laine-Kaulio H, Backnén S, Koivusalo H, Laurén A. 2015. Dye tracer visualization of flow patterns and pathways in glacial sandy till at a boreal forest hillslope. *Geoderma*. **259-260**: 23–34.

Larssen T, Duan L, Mulder J. 2011. Deposition and leaching of sulfur, nitrogen and calcium in four forested catchments in China: implications for acidification. *Environ Sci Technol*. **45**: 1192–1198.

Lehmann P, Hinz C, McGrath G, Tromp-van Meerveld H J, McDonnell J J. 2007. Rainfall threshold for hillslope outflow: an emergent property of flow pathway connectivity. *Hydrol Earth Syst Sci*. **11**: 1047–1063.

Longobardi A, Villani P, Grayson R B, Western A W. 2003. On the relationship between runoff coefficient and catchment initial conditions. *In* MODSIM (ed.) Proceedings of MODSIM 2003 International Congress on Modelling and Simulation. Vol. 1. MODSIM, Townsville. pp. 867–872.

McGlynn B L, McDonnel J J, Brammer D D. 2002. A review of the evolving perceptual model of hillslope flowpaths at the Maimai catchments, New Zealand. *J Hydrol*. **257**: 1–26.

Noguchi S, Tsuboyama Y, Sidle R C, Hosoda I. 2001. Subsurface runoff characteristics from a forest hillslope soil profile including macropores, Hitachi Ohta, Japan. *Hydrol Process*. **15**: 2131–2149.

Ridolfi L, D'Odorico P, Porporato A, Rodriguez-Iturbe I. 2003. Stochastic soil moisture dynamics along a hillslope. *J Hydrol*. **272**: 264–275.

Ritsema C J, Nieber J L, Dekker L W, Steenhuis T S. 1998. Stable or unstable wetting fronts in water repellent soils—effect of antecedent soil moisture content. *Soil Till Res*. **47**: 111–123.

Rosenbaum U, Bogena H R, Herbst M, Huisman J A, Peterson T J, Weuthen A, Western A W, Vereecken H. 2012. Seasonal and event dynamics of spatial soil moisture patterns at the small catchment scale. *Water Resour Res*. **48**: W10544.

Shi H, Chen F Q, Liu S R. 2005. Macropores properties of forest soil and its influence on water effluent in the upper reaches of Minjiang River. *Acta Ecol Sin* (in Chinese). **25**: 507–512.

Sidle R C, Noguchi S, Tsuboyama Y, Laursen K. 2001. A conceptual model of preferential flow systems in forested hillslopes: evidence of self-organization. *Hydrol Process*. **15**: 1675–1692.

Stolte J. 1997. Manual for Soil Physical Measurements. DLO Winand Staring Centre, Wageningen.

Tromp-van Meerveld H J, McDonnell J J. 2006. On the interrelations between topography, soil depth, soil moisture, transpiration rates and species distribution at the hillslope scale. *Adv Water Resour*. **29**: 293–310.

Tromp-van Meerveld I, Weiler M. 2008. Hillslope dynamics modeled with increasing complexity. *J Hydrol*. **361**: 24–40.

Van Genuchten M T. 1980. A closed-form equation for predicting the hydraulic conductivity of unsaturated soils. *Soil Sci Soc Am J*. **44**: 892–898.

Van Genuchten M T, Leij F J, Yates S R. 1992. The RETC Code for Quantifying the Hydraulic Functions of Unsaturated Soils. U.S. Salinity Laboratory, U.S. Department of Agriculture, Agricultural Research Service, Riverside.

Van Reeuwijk L P. 2002. Procedures for Soil Analysis. 6th Edn. International Soil Reference and Information Center (ISRIC), Wageningen.

Van Schaik N L M B, Schnabel S, Jetten V G. 2008. The influence of preferential flow on hillslope hydrology in a semiarid watershed (in the Spanish Dehesas). *Hydrol Process*. **22**: 3844–3855.

Van der Heijden G, Legout A, Pollier B, Bréchet C, Ranger J, Dambrine E. 2013. Tracing and modeling preferential flow in a forest soil – potential impact on nutrient leaching. '*Geoderma*. **195-196**: 12–22.

Wang S M, He Q, Ai H N, Wang Z T, Zhang Q Q. 2013. Pollutant concentrations and pollution loads in stormwater runoff from different land uses in Chongqing. *J Environ Sci*. **25**: 502–510.

Wang W, Zhang H J, Cheng J H, Wu Y H, Du S C, Wang R. 2010. Macropore characteristics and its relationships with the preferential flow in broadleaved forest soils of Simian Mountains. *Chin J Appl Ecol* (in Chinese). **21**: 1217–1223.

Wang Y H. 2012. Characteristics of stand structure and hydrological function of damaged Masson pine forests in the acid rain region of Chongqing (in Chinese). Ph.D. Dissertation, Chinese Academy of Forestry, Beijing.

Wei X, Liu S, Zhou G, Wang C. 2005. Hydrological processes in major types of Chinese forest. *Hydrol Process*. **19**: 63–75.

World Reference Base for Soil Resources (WRB). 2006. World Reference Base for Soil Resources. 2nd Edn. Food and Agriculture Organization of the United Nations, Rome.

Zégre N, Skaugset A E, Som N A, McDonnell J J, Ganio L M. 2010. In lieu of the paired catchment approach: Hydrologic model change detection at the catchment scale. *Water Resour Res*. **46**: W11544.

Zaslavsky D, Rogowski A S. 1969. Hydrologic and morphologic implications of anisotropy and infiltration in soil profile development. *Soil Sci Soc Am J*. **33**: 594–599.

Zhang Z J, Wang Y H, Yu P T, Yuan Y X, Li Z Y, Zhang G Z, Liu Y G. 2008. Characteristics of biomass and root distribution of *Pinus massoniana* with different dominance. *J Nanjing For Univ* (in Chinese). **32**: 71–75.

Zhang Z Q, Wang L X, Wang S P. 2004. Forest hydrology research in China. *Sci Soil Water Conserv* (in Chinese). **2**: 68–73.

Zhu J, Mulder J, Wu L P, Meng X X, Wang Y H, Dörsch P. 2013a. Spatial and temporal variability of N_2O emissions in a subtropical forest catchment in China. *Biogeosciences*. **10**: 1309–1321.

Zhu J, Mulder J, Bakken L, Dörsch P. 2013b. The importance of denitrification for N_2O emissions from an N-saturated forest in SW China: results from in situ ^{15}N labeling experiments. *Biogeochemistry*. **116**: 103–117.